17th Australasian Fluid Mechanics Conference
Auckland, New Zealand
5-9 December 2010

Natural Ventilation Induced by Solar Chimneys

B P Huynh

Faculty of Engineering and IT
University of Technology, Sydney, NSW 2007, Australia

Abstract

Natural-ventilation flow through a two-dimensional but real-sized square room is investigated numerically, using a commercial Computational Fluid Dynamics (CFD) software package. The flow is induced by a solar chimney positioned on the room's roof, and it is desired to have this flow passing through the lower part of the room for ventilation purpose. The chimney in turn is in the form of a parallel channel with one plate kept at a uniform temperature that is higher than that of the ambient air (by up to 40°C), while the other plate and all of the room's walls are insulated. Effects on ventilation flow rate and flow pattern due to a range of changing factors are investigated. The factors include temperature of the chimney's heated plate, length and inclination of the chimney, its location and locations of the room's other openings, and the presence of a vertical partition in the room. It is found that all these factors affect either the flow rate or flow pattern, or both. Maximum flow rate is obtained when solar chimney is in a vertical position at a roof's corner, with its heated plate on the room side. On the other hand, flow rate increases with increasing solar plate's temperature and length, as expected, but the manner of the increase varies with relative positions between the chimney and room inlets.

Introduction

People spend most of their time indoors. A comfortable indoor environment is thus essential for the occupants' good health and productivity. Buildings are responsible for about half of a modern society's total energy consumption. HVAC (Heating, Ventilation and Air-Conditioning), in turn, accounts for a major proportion of this energy demand, thus estimated to be about 68% in non-industrial (commercial and residential) buildings [16]; HVAC is often used to provide thermal comfort to the occupants. Minimising HVAC energy consumption will thus result in great economic benefits. It also contributes beneficially to the issue of sustainable future and climate change, by reducing fuel burning.

Natural ventilation can be used to help reduce significantly HVAC energy demand. A solar chimney (thermal chimney) helps enhance natural ventilation by being heated with solar radiation, causing hot air to rise and inducing the ventilation flow. This device has been much investigated [1-6, 9-10, 12-17]; but there are still many factors affecting its performance (measured by the induced flow rate, for example) not yet considered, especially in building settings. This work investigates computationally natural ventilation induced by roof-mounted solar chimneys through a two-dimensional but real-sized square room. Air-mass-flow rate and flow pattern will be considered in terms of chimney-room configuration, the presence of a vertical partition in the room, chimney's length and inclination, position of the chimney's heated plate, and its temperature.

Modelling and Computation

The flow model is depicted in figure 1. A two-dimensional but real-sized square room of width W = 3m and height H = 3m is considered. Flow is induced by a solar chimney (SC) positioned on the room's roof. The chimney in turn is in the form of a parallel channel with one plate kept at a uniform temperature that is higher than the ambient-air temperature which is assumed to be fixed at 300K (27°C). Two inclination states of the chimney are considered: "inclined" when the chimney is inclined at an angle of 30° above the horizontal (shown in figure 1), and "vertical" when chimney is vertical. When the chimney is inclined, its heated plate can be the lower or upper one; and when the chimney is vertical, its heated plate can be on the left or right. Chimney's length is 1.56m in most cases; but a length twice as long, at 3.12m, is also considered.

Air is induced into the chimney through its lower opening which is a slot on the room's roof either at B (the middle) or C (right corner), and flows out of the chimney through its upper opening. Air enters the room via one or 2 slots located at A (on the roof), D (at bottom of the left vertical wall) or E (bottom of right wall). Opening slots' locations A, B, C, D, and E are shown in figure 1; all slots are 0.3m wide. Note that when SC is inclined, the distance between its 2 plates is only 0.260m [= 0.3cos(30°)]; but when SC is vertical, this distance is 0.3m. Another factor is the presence or absence of a vertical partition which is a thin solid wall hanging down from the roof, ending at 0.3m above the floor. Table 1 shows the various configurations (series) considered. Computational flow domain thus consists of the room's space plus the space between the SC's plates.

All fluid properties are assumed to be constant and corresponding to those of air at 300K (constant ambient temperature T_a) and standard pressure at sea level (101.3kPa); but Boussinesq approximation is also assumed for the buoyancy force arising from density variation as a result of temperature change. The following values of molecular properties are used (using common notation): ρ = 1.161 kg/m^3; μ = 1.846×10^{-5} N-s/m^2; ν = 1.589×10^{-5} m^2/s; k = 0.0263 W/m-K; c_p = 1007 J/kg-K; α = 2.25×10^{-5} m^2/s; Pr = ν/α = 0.707; $\beta = 1/T_a$ = 1/300 K^{-1}. With these values, the Rayleigh number Ra, which is a key parameter in free convection and based on the inclined chimney's internal gap size (0.260m), is Ra = 1.60×10^6(ΔT), where ΔT is the temperature difference between the SC's heated plate and the ambient air. In this work, ΔT can be up to 40°C. Since turbulence is expected at Ra > 10^6 for free convection in similar configurations [11], all cases considered in this work are taken to be turbulent. Following a common practice, turbulent Prandtl number is taken to be constant at 0.9. It should be noted, however, that since laminar flow is a special case of turbulent flow with zero turbulence level, use of a turbulence model (see below) in laminar flow should not affect the computational results' correctness. Thus, for example, with a case from the t series with heated plate's temperature 301K wherein laminar flow is expected in the room, computation with a turbulence model (versus laminar-flow computation) results in a difference of only 0.02% in the air-mass-flow rate through each of the room's inlets.

A Reynolds-Averaged Navier-Stokes (RANS) formulation is used, wherein turbulence affects the mean flow through a turbulent viscosity μ_t; turbulent stresses are assumed to be proportional to the mean rates of strain via μ_t. The low-Reynolds-number K-ε turbulence model of Chien [7] is adopted, where K stands for the turbulent kinetic energy and ε its dissipation rate. Thus, governing equations are those of Reynolds-averaged conservation of mass and momentum, and balance of energy, plus the two transport equations for K and ε of the Chien model.

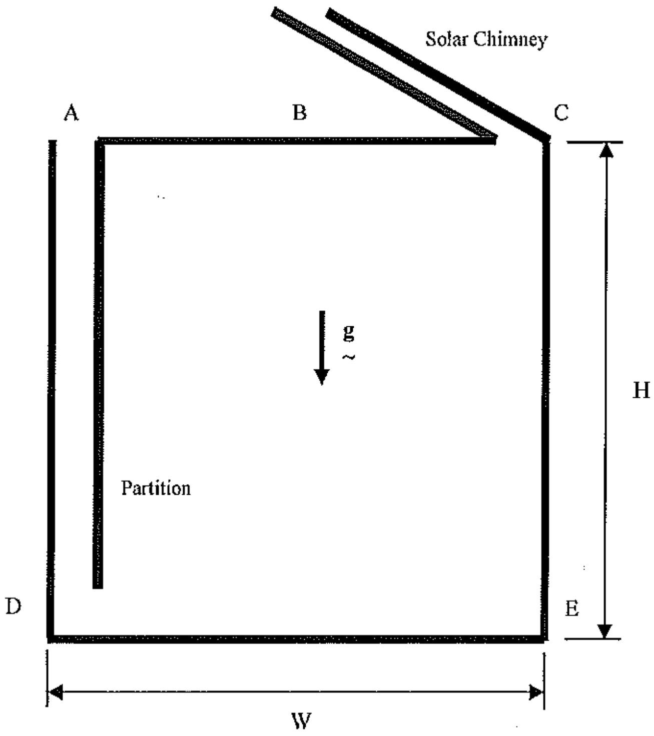

Figure 1. A typical geometry of the 2-dimensional flow model; room size is W × H = 3 m × 3 m; all openings are 0.3m-wide slots.

Referring to figure 1, boundary conditions for the mean variables (velocity components, pressure and temperature) are as follows

- All openings on the flow domain's boundary (SC's upper opening, inlets to the room at A (figure 1), and D and E in some configurations) are prescribed with ambient conditions; the fluid has constant ambient pressure and temperature, namely p = 0 (gauge, without the hydrostatic component), $T = T_a$ = 300K. However, the thermal condition here applies only on those sections of an opening where there is inflow; if the computation reveals outflow on any sections, the constant temperature condition there will be ignored; instead, temperature will be computed. Similarly, the constant pressure condition applies only on those sections of an opening where there is outflow; if the computation reveals inflow on any sections, the constant pressure condition there will be ignored, and pressure will be computed instead
- Isothermal wall condition is prescribed to the heated plate of the chimney: zero velocity, $T = T_{plate}$ (constant, and $> T_a$)
- All other solid surfaces (walls, roof and floor of the room, SC's non-heated plate, and the partition when it is present) are adiabatic walls: zero velocity; $\partial T/\partial n = 0$

The turbulence-model variables K and ε are prescribed as follows

- On all solid surfaces: default solid-surface condition of the software package (see below) is adopted; this entails K = 0 and ε = 0, following Chien [7]
- At all openings, K and ε are assumed to be constant. However, these conditions apply only on those sections of an opening where there is inflow; if the computation reveals outflow on any sections, the prescribed values for K and ε there will be ignored; instead, these will be computed. It is found that the small turbulence level prescribed on the openings has very small effects on the results. For example, when an arbitrary value of $K = 1\times10^{-5}$ m^2/s^2 and $\varepsilon = 1\times10^{-5}$ m^2/s^3 are prescribed, the air-mass-flow rate varies by less than 0.3% from when K and ε are both zero. From considerations similar to this, $K = 1\times10^{-5}$ m^2/s^2 and $\varepsilon = 1\times10^{-5}$ m^2/s^3 are used on all openings.

Series	Partition	Inlet location	SC location	SC inclination	SC's heated plate
d	Yes	A	C	inclined	Lower
e	No	A	C	inclined	Lower
g	No	D	C	inclined	Lower
h	No	E	C	inclined	Lower
i	No	D & E	C	inclined	Lower
l	No	A	C	vertical	Left
m	No	A	C	vertical	Right
t	No	D & E	B	inclined	Lower
u	No	D	B	inclined	Lower
x	No	D & E	B	inclined	Upper
y	No	A	C	inclined	Upper
z	No	E	C	inclined	Upper
b*	No	A	C	inclined	Lower

Table 1. Series (configuration) of the cases considered. In each series temperature of the solar chimney (SC)'s heated plate is varied. SC's length is 1.56m, except for series b* wherein this length is 3.12m.

The commercial Computational Fluid Dynamics (CFD) software package CFD-ACE from the ESI Group is used for the computation. The package is quite well known, and its validation is thus assumed to have been adequate. Some further tests had also added positively to its validity [8]. Numerical scheme is the Finite Volume method, and the coupled system of governing equations is solved iteratively for the two mean velocity components, mean temperature and pressure, plus K and ε. Both upwind and central-difference differencing schemes are used. A convergence criterion of reduction of residuals in the solved variables by 3 orders of magnitude is adopted. This is adequate; comparison of the solutions with residual reduction of 3 orders of magnitude and those with 4 orders of magnitude shows very small difference. For example, with a test case from series u with plate temperature 310K, the above change of convergence criterion results in the air-mass-flow rate changing by only 0.0013%. Computation is done with 64-bit precision.

Grid convergence tests have also been performed to ascertain the adequacy of the grid patterns used. For example, with a case from t series with plate temperature 320K, as the number of grid points on each edge (see figure 1) is increased by 20% (resulting in 44% increase in the number of 2-D computational cells), change in the net mass in-flow to the room is only 0.41%. From this and similar tests, patterns with 300×360 grid points for the room (300 in the vertical direction) and 60×160 for the chimney (60×320 for the long chimney of series b*) are used. Also, post-solution checks of values of y^+, the non-dimensional distance from closest wall, of grid points closest to the walls show y^+ being well below 1, thus confirming that the grid patterns used are sufficiently fine for the Chien turbulence model.

Results and Discussion

Air-mass-flow rate and flow pattern have been considered for a range of configuration of the flow domain, and temperature of the chimney's heated plate. The configuration's factors include length and inclination of the chimney, its location and locations of the room's other openings, and the presence of a vertical partition in the room. The considered configurations (series) are shown in table 1. Location of the chimney refers to location of the opening slot on the room's roof, which is also the lower entrance to the chimney. In all series, SC's length is 1.56m [= (3 − 0.3)/(2cos30°)], except for series b* wherein this length is twice as long, at 3.12m.

Figure 2 shows the net air-mass-flow rate m in terms of the temperature difference ΔT between the chimney's heated plate and ambient air, for different configurations (series). On log-log scales, the m-versus-ΔT curves are nearly straight lines, but with different slopes. The highest flow rates occur when chimney is located at a roof corner and inlet to the room at the opposite roof corner (series d, e), but only at sufficiently high ΔT (in contrast to low-ΔT results indicated by y-series). With inlets to the room at its lower corners, there is little difference in m (series t, h, u and z); 2 inlets (series t) give slightly more flow than a single inlet (series u); similarly with series i versus g (shown in figure 3). That maximum flow rates occur with series d and e is believed to be due to the longer and not-so-twisted flow path (as in series h, z) from room's inlets to the chimney, resulting in stronger stack effect (flow pattern is shown in figure 4).

Figure 2 also shows that a partition reduces m slightly (series e versus d). This agrees with expectation, as partitions offer extra resistance to the fluid motion.

Figure 3 shows an increasing m with configuration for ΔT = 20°C. Values from series z versus h (figure 2) and x versus t indicate that a slightly higher m is obtained when chimney's upper plate is heated. But when chimney is upright, a left heated-plate (on the room side, series l) gives a much higher flow rate than the right one (series m, whose flow pattern (figure 4) shows much more back-flow at chimney exit than series l (not shown)). Series l gives maximum flow rate, much larger than that from series d and e. This is believed to be due to a taller vertical height rather than a larger internal passage, however. It's interesting to note that air flow in series l would be sufficient to supply an amble rate of 8 l/s to 19 persons in a room of 5-m length.

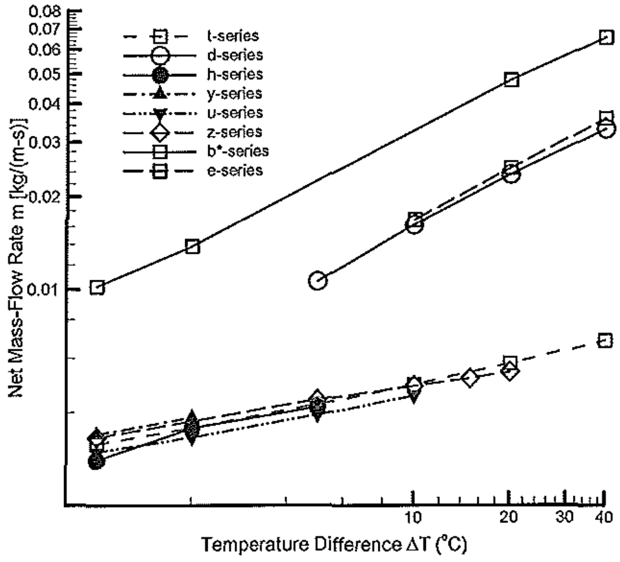

Figure 2. Net air-mass-flow rate m versus temperature difference ΔT between the solar chimney (SC)'s heated plate and ambient air.

Readings from series e and b* show that doubling the chimney's length results in near double in flow rate; thus m is nearly proportional to chimney's length.

Flow patterns corresponding to a number of series are shown in figure 4, with ΔT = 20°C. Note that in this figure, the horizontal and 2 vertical lines inside the room should be disregarded (except for the section of the vertical line corresponding to the partition at A (see figure 1) when this is present); these lines are used in the discretisation of the computational domain, and thus are not part of the solution contours. The figure shows that the presence of a partition (series d) results in the lower part of the room being ventilated better. This is often a very desirable aspect in ventilation. This and other similar figures (not shown) also indicate that when there is significant back-flow at the chimney's exit, flow rate is correspondingly low; an example is series m (versus series l).

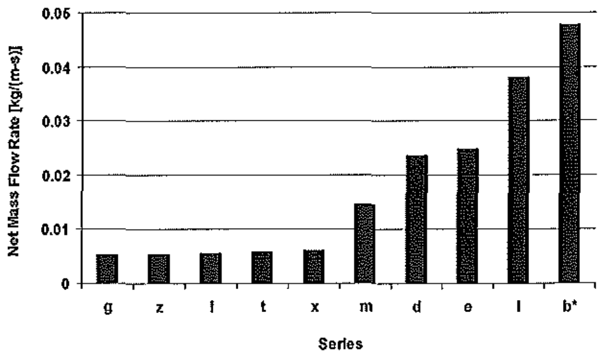

Figure 3. Net air-mass-flow rate m versus configuration (series) of the flow domain, for ΔT = 20°C.

Conclusions

Natural ventilation induced by solar chimneys through a two-dimensional but real-sized square room has been investigated numerically. Net air-mass-flow rate m through the room is seen to increase with temperature of the chimney's heated plate; the increase follows approximately straight lines on log-log scales but with different slopes for different configurations. m is also affected to varying degree by factors like location of the chimney and of the room's other openings, which of the chimney's two plates that is heated, length and inclination of the chimney, and the presence of a vertical partition in the room. Largest flow rate occurs in series l when a vertical chimney is positioned at a corner of the room's roof, while inlet to the room is at the opposite corner and chimney's heated plate being on the room side. Doubling the chimney's length results in near double in flow rate in one considered configuration. A partition reduces m only slightly, but helps ventilate the lower part of the room better.

References

[1] Afonso, C. & Oliveira, A., Solar Chimneys: Simulation and Experiment, *Energy and Buildings*, 32, 2000, 71-79.

[2] Bacharoudis, E., Vrachopoulos, M., Koukou, M. & Filios, A., Numerical Investigation of the Buoyancy-Induced Flow Field and Heat Transfer Inside Solar Chimneys, *Proc. 2006 IASME/WSEAS Intern. Conf. on Energy & Environmental Systems*, Chalkida, Greece, 8-10 May 2006, 293-298.

[3] Bansal, N.K., Mathur, J., Mathur, S. & Jain, M., Modeling of Window-Sized Solar Chimneys for Ventilation, *Building and Environment*, 40, 2005, 1302-1308.

[4] Bansal, N.K., Mathur, R. and Bhandari, M., Solar Chimney for Enhanced Stack Ventilation, *Building and Environment*, 28, 1993, 373-377.

[5] Bassiouny, R. and Korah, N.S.A., Effect of Solar Chimney Inclination Angle on Space Flow Pattern and Ventilation Rate, *Energy and Buildings*, 41, 2009, 190-196.

[6] Bassiouny, R. and Koura, N.S.A., An Analytical and Numerical Study of Solar Chimney Use for Room Natural Ventilation, *Energy and Buildings*, **40**, 2008, 865-873.

[7] Chien, K.-Y., Predictions of Channel and Boundary-Layer Flows with a Low-Reynolds-Number Turbulence Model, *AIAA Journal*, **20**, 1982, 33-38.

[8] Huynh, B.P., Free Convection Cooling of a Horizontal Cylinder Positioned Above a Plane, *Proc. 13th Intern. Heat Transfer Conf.*, Sydney, Australia, 13-18 August 2006.

[9] Khedari, J., Boonsri, B. and Hirunlabh, J., Ventilation Impact of a Solar Chimney on Indoor Temperature Fluctuation and Air Change in a School Building, *Energy and Buildings*, **32**, 2000, 89-93.

[10] Lee, K.H. and Stand, R.K., Enhancement of Natural Ventilation in Buildings Using a Thermal Chimney, *Energy and Buildings*, 41, 2009, 615-621.

[11] Markatos, N.C. and Pericleous, A.K., Laminar and Turbulent Natural Convection in an Enclosed Cavity, *Intern. J. Heat & Mass Transfer*, **27**, 1984, 755-772.

[12] Marti-Herrero, J. and Heras-Celemin, M.R., Dynamic Thermal Simulation of a Solar Chimney with PV Modules, *Proc. Intern. Conf. "Passive & Low Energy Cooling for the Built Environment"*, Santorini, Greece, May 2005, 891-896.

[13] Mathur, J., Bansal, N.K., Mathur, S., Jain, M. and Anupma, Experimental Investigations on Solar Chimney for Room Ventilation, *Solar Energy*, **80**, 2006, 927-935.

[14] Mathur, J., Mathur, S. and Anupma, Summer-Performance of Inclined Roof Solar Chimney for Natural Ventilation, *Energy and Buildings*, **38**, 2006, 1156-1163.

[15] Ong, K.S. and Chow, C.C., Performance of a Solar Chimney, *Solar Energy*, **74**, 2003, 1-17.

[16] Orme, M., Estimates of the Energy Impact of Ventilation and Associated Financial Expenditures. *Energy and Buildings*, **33**, 2001, 199-205.

[17] Thong, T.B., Quaan, L. & Ong, K.S., Simulation of Flow in a Solar Roof Collector Driven by Natural Convection, *Proc. 16th Australasian Fluid Mech. Conf.*, Gold Coast, Australia, 2-7 December 2007.

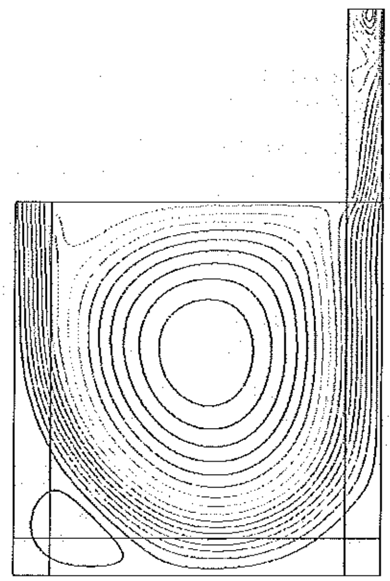

(i)

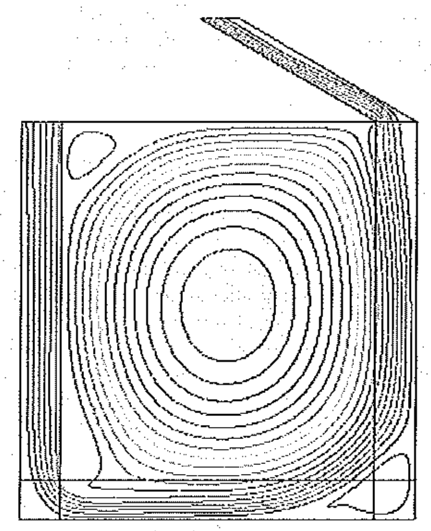

(ii)

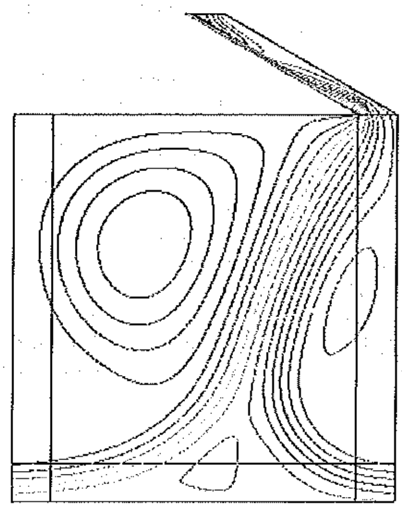

(iii)

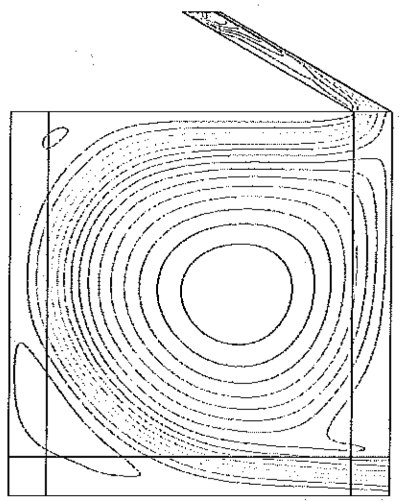

(iv)

Figure 4. Flow pattern of some representative series, with $\Delta T = 20°C$; (i) series m; (ii) series d; (iii) series i; (iv) series z.

17th Australasian Fluid Mechanics Conference

Auckland, New Zealand
5 - 9 December 2010

Welcome
Sponsors
Committee
AFMS Information

Papers
Reviewed Abstracts
Author Index
Search
Conference Programme

Edited by Prof. G.D. Mallinson and Dr J.E. Cater

Presented by the Faculty of Engineering
in association with the Centre for Continuing Education
The University of Auckland

ISBN: 978-0-86869-129-9

17th Australasian
Fluid Mechanics Conference

Auckland, New Zealand
5 - 9 December 2010

Welcome

The Organising Committee of the 17th Australasian Fluid Mechanics Conference would like to take the opportunity to welcome you to New Zealand, to Auckland and to the 17th meeting of this conference.

The Australasian Fluid Mechanics Conferences have been held triennially since the series inception as the Australasian Hydraulics and Fluid Mechanics Conference at the University of Western Australia 1962. This Conference is the 17th meeting, the 4th of the series to be held in New Zealand, and the 3rd to be held at The University of Auckland. These conferences, at which all contributions are presented orally, have the tradition of providing graduate students with an opportunity to interact with a community of richly experienced researchers, and have played a very significant role of nurturing fluid mechanics research in Australasia and the surrounding region for nearly four decades.

The role of developing this vibrant community has been formalised with the recent formation of the Australian Fluid Mechanics Society, and this is the first event which has been associated with the AFMS. A highlight of this meeting will be the celebration of the induction of the 10 inaugural AFMS Fellows at the conference banquet.

A feature of the AFMC series is the broad range of fluid mechanics research presented, and this conference is no different as evidenced by the 28 themes identified in the programme, the 235 presentations and over 200 papers submitted. The flavour of a particular meeting is set by the plenary speakers and the conference committee is very grateful for the contributions of David Boger, Vladimir Nikora, Mike O'Sullivan, Andrew Pollard and Phil Schwarz for providing high quality thematic foci.

As Chair I would like to acknowledge here the efforts of John Cater the conference secretary and the other members of the conference Organising Committee; Rosalind Archer, John Chen, Richard Clarke, Stephen Coleman, Richard Flay, Bruce Melville, Roger Nokes, Stuart Norris, Peter Richards and Rajnish Sharma. I also acknowledge the 120 reviewers of the abstracts and papers. The Committee would particularly like to thank Tessa Hagemann, of the Conference Management unit in The University of Auckland's Centre for Continuing Education who has tirelessly provided the administrative support that has allowed the committee to concentrate on the technical aspects of the conference.

Finally, the Committee would also like to acknowledge the support of the Faculty of Engineering at The University of Auckland and the Conference sponsors: the platinum sponsor Olympus, COMSOL Multiphysics, LasTEK & LaVision, LEAP Australia, Kenelec Scientific, Duff and Macintosh, New Spec & Spectra-Physics.

Gordon Mallinson
Chair

17AFMC Programme Timetable

Monday

09:00-09:30: Welcome

09:30-10:30: The GK Batchelor Lecture - David Boger

10:30-11:00: Coffee

11:00-13:00 Technical Sessions 1	CFD I - Aero-hydrodynamics Plenary Theatre 260-098		Microfluidics Case Room 2		Active Flow Control I Case Room 3		Heat Transfer I Case Room 4		Wind Energy Theatre OGGB3	
Paper	38	Numerical and Experimental Investigation of Helicopter Fuselage Aerodynamics	75	Computational study of flow in a micro-sized hydrocyclone	35	The influence of forcing frequency and amplitude to effectiveness of synthetic jets on laminar separation control	40	Flow Distribution in Large Area Building Integrated Solar Collectors	24	Performance of a model wind turbine
Presenting Author		Mr Rhys Lehmann		Mr Guofeng Zhu		Dr Guang Hong		Dr Tim Anderson		Dr Per-Åge Krogstad
Paper	185	Numerical simulation of three-dimensional wind flow around grain storage bunkers	128	Slip MHD flow over permeable stretching surface with chemical reaction	64	Turbulent drag reduction using an array of piezo-ceramic actuators	58	Effect of surface roughness on small-scale velocity and scalar characteristics in a turbulent channel flow	181	A wind-tunnel investigation of the wake behind a wind-turbine in a turbulent boundary-layer flow using stereo-PIV
Presenting Author		Mr Wei He		Mr Mohammad Hossein Yazdi		Prof Yu Zhou		Prof Robert Antonia		Dr Steve Cochard
Paper	251	The effect of wing corrugations on the aerodynamic performance of low-Reynolds number flapping flight	161	Micro PIV analysis of secondary vortices with observations of primary vortices in single bubble cavitation microstreaming	136	Arrangement of Actuators for Active Laminar Flow Control	68	Modelling of Heat and Mass Transfer Involving Vapour Condensation in the Presence of Non-Condensable Gases	190	Advances In Computational Fluid Dynamics For Modelling Wind Flow Over Complex Terrain
Presenting Author		Miss Sarah Premachandran		Mr James Collis		Mr Patrick Kenny		Mr Mohammad Saraireh		Mr John O'Sullivan
Paper	253	Development of a CFD model for an oscillating hydrofoil	325	A Micro Particle Image Velocimetry System for Velocity Field Measurement in a Microchip Droplet-Forming Flow	207	Control of Convective Rolls by Spatially Distributed Wall Heating	96	Flow visualization to determine the flow structure in a vortex tube	287	Turbulence effects on wind flow over complex terrain
Presenting Author		Suzanne Hutchison		Dr Ilija Sutalo		Dr Jerzy M. Floryan		Mr Yunpeng Xue		Mr Michael Sherry
Paper	327	Numerical Simulation of a Supersonic Convergent Divergent nozzle with divergent angle variations for Underexpanded condition	331	Oxygen Sensor Using a Gas-Liquid Mass Transfer in Microchip	211	Fluidic Modulation of Nozzle Thrust.	180	Natural Convection in a Wedge-Shaped Domain Induced by Constant Isothermal Surface Heating	359	Wind Tunnel Testing Of A Wind Turbine With Telescopic Blades
Presenting Author		Ms Sudharshani Ekanayake		Dr Chuanpin Chen		Mr Ashraf Ali		Assoc Prof Chengwang Lei		Dr Rajnish Sharma
Paper	42	Three-dimensional numerical simulation of hydrodynamic forces on an oblique cylinder in oscillating flow	353	A Two-sided Model for Droplet Spreading and Evaporation on Semi-confined Geometries			230	Modeling of radiating flows in the atmospheres of the gas giants	321	Wind Turbine Wake Modelling using Large Eddy Simulation
Presenting Author		Mr Ming Zhao		Mr Laith Hurmez				Prof Richard Morgan		Dr Stuart Norris

13:00-14:00: Lunch

14:00-15:00: Plenary: Mike O'Sullivan

15:00-15:30: Tea

15:30-17:30 Technical Session 2	CFD II - Methodologies Plenary Theatre 260-098		Geothermal Case Room 2		Active Flow Control II Case Room 3		Heat Transfer II Case Room 4		Wind Engineering / Atmospheric Physics Theatre OGGB3	
Paper	105	Hybrid volume-of-fluid and discrete particle solver for oil-mist filter simulations	345	Improving the performance of natural draft cooling towers for application in geothermal power plants	222	LES of a Low Velocity-Ratio Jet in a Flat Plate Turbulent Boundary Layer	198	A Thermodynamic Model for a High-Pressure Hydrogen Gas Filling System Comprised of Carbon-Fibre Reinforced Composite Pressure Vessels	76	Covariance integration approach to the determination of influence coefficients of internal pressure in a low rise building
Presenting Author		Dr Andrew King		Dr Kamel Hooman		Dr James Jewkes		Dr Peter Woodfield		Mr Tushar Kanti Guha
Paper	116	Viscosity and validity of a kinetic theory based flow modelling scheme	352	Development of a New Correlation for Measuring Two-Phase Flow in Geothermal Pipelines using Orifice Plates	231	Flow control in micro-channels using groove orientation	225	Fluid flow and thermal characteristics in a microchannel with cross-flow synthetic jet	212	Steady Aerodynamics of Rod and Plate Type Debris
Presenting Author		Mr Chin Wai Lim		Sadiq Zarrouk		Dr Jerzy M. Floryan		Prof Tilak Chandratilleke		Dr Peter Richards
Paper	139	Simulation of Fluid Flows at High Reynolds Numbers Using Integrated Radial Basis Functions	393	Reinjection at Wairakei Tauhara Geothermal Field	255	Accuracy of instantaneous flow rate estimation using pressure measurements	257	The Use of Thermochromic Liquid Crystals to Investigate Heat Transfer Enhancement in a Channel with a Protrusion	262	An Experimental Study of Wind Force Acting on Commercial Double-Layered Square Metal Meshes at Different Spacing
Presenting Author		Dr Nam MAI-DUY		Ms Eylem Kaya		Ms Ayaka Kashima / Dr Pedro Lee		Dr Osama Alshroof		Dr Ahmad Sharifian
Paper	172	Intersection Marker (ISM) method for tracking a deformable 2D surface in 3D Eulerian Space	390	Large-Scale Natural Convection in the Wairakei-Tauhara Geothermal Field	275	Frequency selection in time-dependent open flows	291	Natural ventilation induced by solar chimneys	141	Two-point Correlation Statistics in the Atmospheric Surface Layers
Presenting Author		Mark Ho		Ms Emily Clearwater		Dr Justin Leontini		Dr Ba Phuoc Huynh		Dr Kapil Chauhan
Paper	229	Simulations of supersonic flows using new kinetic scheme based on the free-molecular-type equation	361	Medium- and Fluid-Compressibility Effects in Flows through Hot Sedimentary Aquifers	350	Quasi-2D simulation of liquid metal flow past a cylinder in a duct exposed to a magnetic field	363	The stability of conjugate natural convection boundary layers	151	Radiative instability of vortices in a stratified fluid
Presenting Author		Dr Takeshi Kataoka		Dr Simon Marshall		Mr Wisam Al-Saadi		Dr Nicholas Williamson		Dr Patrice Meunier
Paper	298	Analysis of the Anisotropy of Finite Difference Schemes	358	Dynamic model development of a Brayton-cycle based power-loop for a geothermal power plant	362	Minijet-controlled turbulent round jet				
Presenting Author		Dr Andrew Ooi		Mr Rajinesh Singh		Prof. Jianchun Mi				